

## Pipeline upheaval buckling in clayey backfill using numerical analysis

<sup>1\*</sup>A. Koochekali; <sup>2</sup>B. Gatmiri; <sup>3</sup>A. Koochekali

<sup>1</sup> College of Engineering, University of Tehran, Enghelab sq. Tehran, Iran

<sup>2</sup> University of Tehran, Enghelab sq. Tehran, Iran

<sup>3</sup> Department of Civil Engineering, Islamic Azad University, Science and Research branch, Tehran, Iran

Received 10 February 2013; Revised 9 March 2013; Accepted 7 May 2013

**ABSTRACT:** Offshore pipelines used for oil and gas transportation are often buried to avoid damage from fishing activities and to provide thermal insulation. Thermal expansion and contraction of the pipeline during operation can lead to lateral or upheaval buckling. A safe buried pipeline design must take into account a reliable evaluation of soil uplift resistance and pipe embedment depth. While the cost of burying a pipeline for tens or hundreds of kilometer is significant, it is important to optimize the required soil cover depth. In this paper a parametric study of pipeline upheaval buckling in clayey backfill has been conducted using finite element analysis. Three different embedment depths are considered. Uplift resistance is calculated and failure mechanism is obtained. To simulate the large penetration of the pipe into clayey backfill a novel Arbitrary Lagrangian Eulerian (ALE) finite element technique was employed in this paper. The results reveal that as embedment depth increases, uplift resistance increases and also uplift mechanism changes. However, uplift resistance differ less than 5% for deep embedment case. In addition, the amount of pore pressure is investigated beneath the pipe for deep embedment cases and it reveals that negative excess pore pressure occurs under the pipeline.

**Keywords:** *Arbitrary Lagrangian-Eulerian analysis; Embedment depth; Subsea Pipeline; Uplift Mechanism; Uplift Resistance*

### INTRODUCTION

Offshore pipelines used for oil and gas transportation are often buried to avoid damage from fishing activities and to provide thermal insulation. To ease the flow, pipelines operate at high temperature and high pressure. These operating conditions cause thermal expansion in the pipeline, which is restricted by friction at the soil-pipe interface and the end connections. As a result, the buried pipeline has a high vulnerability to vertical movement which is known as upheaval buckling. Due to passive resistance of the trench walls, the pipeline is sufficiently restricted in the lateral direction. The design of a buried pipeline requires the minimum depth of soil cover that will provide sufficient uplift resistance to be determined. Therefore, it is necessary to evaluate the uplift resistance toward this movement. Predicting upheaval buckling resistance of buried pipelines has been a challenge as there is a huge uncertainty and randomness in the nature of soil cover created by various pipe burying techniques (Thusyanthan and Genesan, 2008) Present

understanding on uplift resistance of buried pipe lines is based on analysis of (Maltby and Calladine, 1995; Randolph and Houlsby, 1984) and experimental and centrifuge works by researchers (Baumgard, 2000; Bransby *et al.*, 2002; Cheuk *et al.*, 2007a, 2008b, 2008c; Dickin, 1994; Finch, 1999; Moradi & Craig, 1998; Schaminée *et al.*, 1990; Thusyanthan *et al.*, 2008 and White *et al.*, 2001a, 2008b).

Bransby *et al.* (2002) provided a centrifuge model and evaluated uplift resistance in liquefied clay. Recently, Cheuk *et al.*, (2008a) worked on a centrifuge model in which effects of time after jetting and uplift rate on uplift resistance were assessed on very soft clay. In addition, Merifield *et al.* (2008) and Newson and Deljoui, (2005) provided numerical solutions to evaluate soil uplift and lateral resistance. An uplift force  $W_t$  (per unit length of the pipe) is required to move the pipe vertically upwards, so that it exceeds its capacity (i.e. the soil-pipeline system fails). In general, for a given pipe this 'total ultimate uplift' force,  $W_t$  can be defined as:

$$W_t = W_u + W_p \quad (1)$$

\*Corresponding Author Email: [alayar.kocheh@ut.ac.ir](mailto:alayar.kocheh@ut.ac.ir)  
Tel.: +989122834079

Where  $W_t$  is the total ultimate uplift capacity per unit length of pipe,  $W_u$  is the net ultimate uplift capacity per unit length of pipe (soil resistance to pipe movement), and  $W_p$  is the effective self-weight of the pipe per unit length. The net ultimate uplift capacity ( $W_u$ ) is the focus of the current study, as it varies with embedment depth. Models to predict the uplift capacity of pipelines either consider fully drained conditions or fully un-drained conditions (Schaminée et al., 1990)

For un-drained soil conditions and a pipe which is shallowly embedded, the global failure mode can happen. In this mechanism soil above the pipe will displace upwards when the pipe moves upward. The upheaval buckling resistance can be expressed as a function of the weight of the wedge of the soil above the pipeline and the un-drained shear strength mobilized to each side of this wedge using the similar mechanism shown in Fig. 1a. The simple mechanism gives the uplift capacity

$$\frac{W_u}{\gamma HD} = 1 + 0.1 \frac{D}{H} + \frac{2c_u}{\gamma H} \left( \frac{H}{D} + \frac{1}{2} \right) \quad (2)$$

Where  $C_u$  is the average un-drained shear strength in the vertical slip planes.

Another uplift method for un-drained soil is local failure. In this mechanism soil above pipe will displace around and below the pipe (Randolph and Houlsby, 1984) and a gap does not form beneath the pipeline (Fig. 1b). This is likely to occur for deep pipelines and even moderately buried pipelines in un-drained conditions. For this case the uplift force is:

$$W_u = N_p \cdot c_u \cdot D \quad (3)$$

Where  $C_u$  is un-drained shear strength and  $N_p$  is a capacity factor.

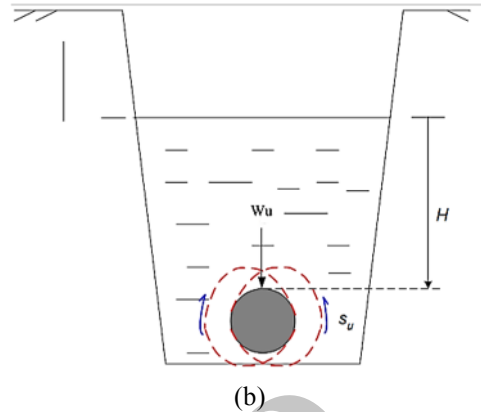
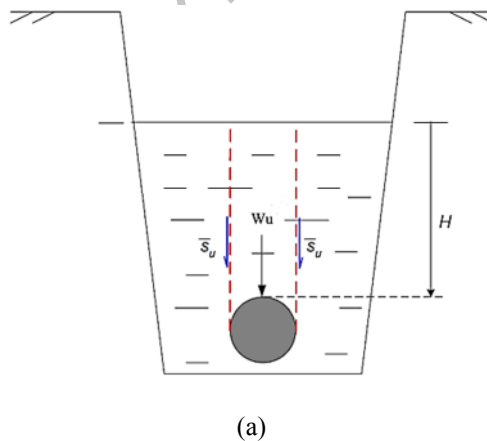


Fig. 1: Uplift mechanism during upheaval buckling, (a) global mode and (b) local mode (Bransby et al. 2002)

Penetration problems in geomechanics involve the insertion or intrusion of solid bodies into the ground. Such problems are extremely difficult to model numerically, because they usually involve severe mesh distortion caused by large deformation and frictional contact. (Sheng et al., 2009) In this paper, an Arbitrary Lagrangian–Eulerian method is used to overcome the mesh distortion problem. The ALE technique is a mesh technique in that a new mesh is created at a certain frequency during the analysis and the solution variables transferred from the original mesh to the new mesh. However, in common ALE implementation, the new mesh must maintain the same topology in terms of elements and connectivity as the original mesh. In other words, the new mesh is obtained by moving the nodes of the original mesh without altering the element connectivity (THO et al., 2012). An advection algorithm is employed to transfer the solution variables from the original mesh to the new mesh Fig. 2. shows general procedure of ALE relocation method.

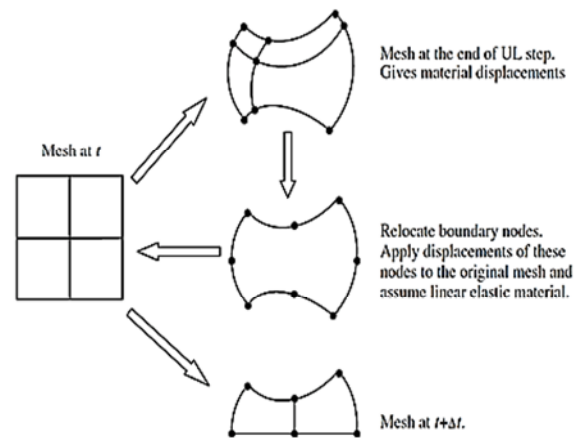


Fig. 2: General Procedure of the ALE node relocation method (Sheng et al., 2009)

In this study, the soil–pipeline interactions under upward movements in soft clay are investigated with particular attention to the peak forces exerted on the pipe. The pull out forces and failure mechanisms for varying pipe embedment depth are investigated. In addition, the amount of excess pore pressure is calculated under the pipe. The pipe penetration problem is solved using ALE finite element technique. The results obtained from this study have been compared with the available analytical solutions. This research is carried out at University of Tehran from May-2011 since May-2012

## MATERIALS AND METHODS

### Finite Element Modeling

#### Geometrical characteristics of analyzed models

Two dimensional plane strain finite element analysis of pipeline uplift was conducted using the displacement finite element software "ABAQUS/CAE 6.10-1". An Arbitrary Lagrangian-Eulerian (ALE) remeshing algorithm was employed during the large soil deformation to allow for geometric nonlinearities. The ABAQUS model consisted of two parts: the pipe and the soil. A typical mesh for this problem, along with the applied displacement boundary conditions, is shown in Fig. 3. The actual distribution and concentration of elements varied as a function of the pipe embedment depth. The mesh is finer around pipe and would be expanded toward boundaries. The pipe is buried in three different depths.

Undrained soil condition is assumed and the soil is modeled as an isotropic elasto-perfectly plastic continuum with failure described by the Mohr–

Coulomb yield criterion. The elastic behavior is defined by a Poisson's ratio of  $\nu = 0.495$ , and Young module  $E = 4000$  kPa and a ratio of Young's modulus to shear strength of  $E/c_u = 400$ . The pipe is assumed as a rigid body and is simulated as a discrete rigid. However, to evaluate effect of this assumption on soil resistance, the pipe is modeled as a two dimensional continuum element either. The pipe elastic behavior is defined by a Poisson's ratio of  $\nu = 0.3$ , and Young module  $E = 10e7$  kPa.

### Element type and Boundary conditions

To assess the amount of pore pressure a "pore fluid/stress" element is implemented. As a result, a typical CPE4P element, 4-noded quadrilateral plane strain elements is used. The deformable pipe is also simulated by CPS4R element, 4-noded quadrilateral plane stress reduced integration.

A frictionless contact is assumed in tangible direction and a hard contact is implemented in normal direction. The separation is allowed between pipe and the soil in this case. At the contact with soil, the poro-elastic elements shared the same nodes with the soil. In addition, the element nodes do not be located at the symmetric line. The total resistance force,  $W_u$ , is calculated by summing the forces at the nodal points in the immediately adjacent to the all sides of the pipe. It is assumed that seabed sea mean water level is 20 meter above the seabed where the pipe is buried. As a result, effect of sea water pressure is considered at seabed boundary condition. The pipe is displaced vertically upward until failure happens. The Pipe is moved upward with an even pace up to 8 centimeter.

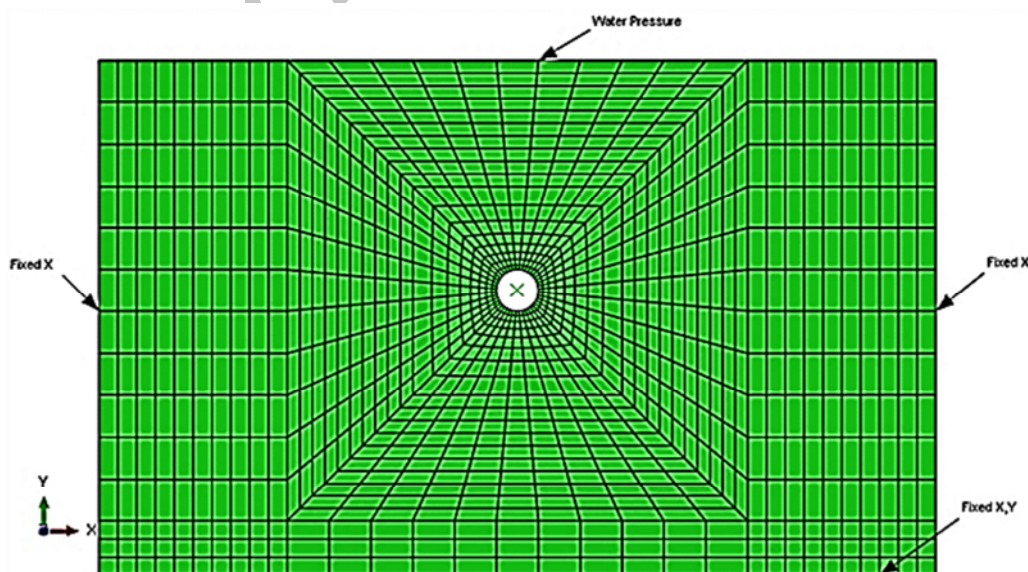


Fig 3: The Mesh geometry and boundary conditions in the Finite element model

*Embedment depth*

To investigate effects of pipe burial depth on uplift resistance and uplift mechanism, three different embedment ratio was considered:  $H/D=1, 5,$  and  $10$  which  $H$  is pipe burial depth and  $D$  is pipe diameter and is equal to 26 centimeter. Table 1 describes these cases.

Table1: Different Normalized Pipe Embedment Depth (Burial Depth/ Pipe Diameter)

Model name	Normalized embedment depth (H/D)
M-1	1
M-5	5
M-10	10

*Finite Element Results*

*Uplift resistance and mechanism*

The uplift resistance for three different cases is plotted against dimensionless pipe displacement ratio in Fig. 4. in which Displacement ratio is equal to ratio of pipe displacement to pipe diameter.

*Deep embedment case*

M-5 and M-10 models are considered as deep embedment case in that flow around mechanism occurs around the pipe in which soil particles flow around the pipe. Results show that uplift resistance changes less than 5% for embedment depth of  $H/D=5, 10$ . As a result, by increasing the embedment depth above 5 no tangible increase in uplift resistance happens. The net uplift force increases linearly at very small displacements up to a pipe displacement of  $0.03D$ . Beyond this linear regime, the uplift force keeps increase but with a decreasing stiffness in the

load-displacement response. The uplift resistance reaches a peak value at pipe displacement of  $0.07D$ . The normalized uplift force or uplift factor  $N_p (=W_u/C_u.D)$  is also calculated. The value of  $N_p$  is equal to 10.8, 11 for M-5 and M-10 cases. Soil displacement around the pipe is observed in Fig.5.a. This figure reveals that surrounding soil would flow around the pipe and flow around mechanism (Randolph and Houlsby, 1984) or local failure mode occurs. The soil plastic strain is also shown in Fig. 5.b.

*Shallow embedment case*

The pipe embedment depth of  $H/D=1$  is called shallow embedment case. Soil displacement during the pipe movement is shown in Fig. 6a. In this case soil particles move upward rather than flowing around the pipe. As a result, global failure mode occurs.

The soil uplift resistance in this case is 8908.8 Pa which is considerably lower than uplift resistance obtained by M-5 and M-10. The net uplift force increases linearly at very small displacements up to a pipe displacement of  $0.03D$ . After that uplift force keeps increasing but with a decreasing stiffness in the load-displacement response. The uplift resistance reaches a peak value at pipe displacement of  $0.15D$ . In this type of failure, global failure, only upper half of pipe would be involved in mobilizing the soil resistance. As a result,  $W_u$  was calculated by summing the forces at the nodal points in the immediately adjacent to upper half of the pipe. The results shows soils at seabed level are displaced upward up to 4 centimeter. The soil plastic strain is also shown in Fig. 6.b.

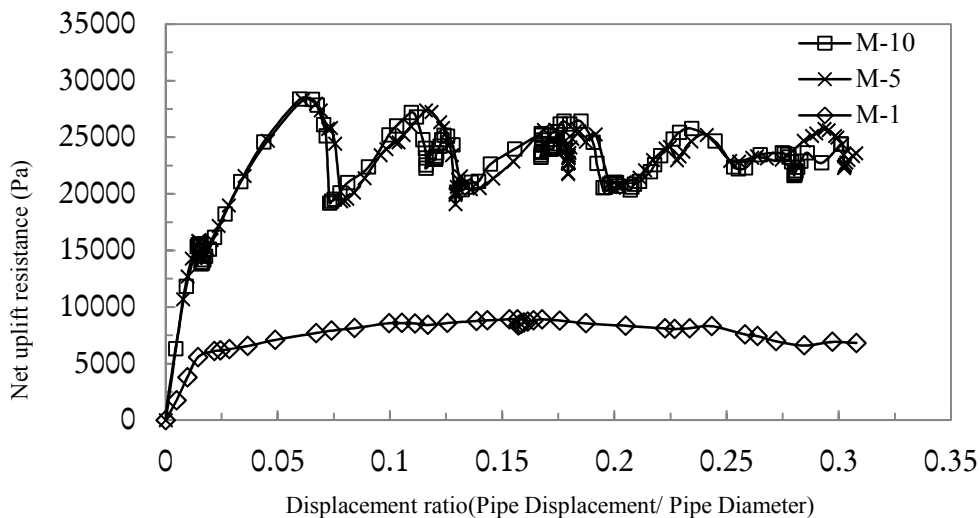
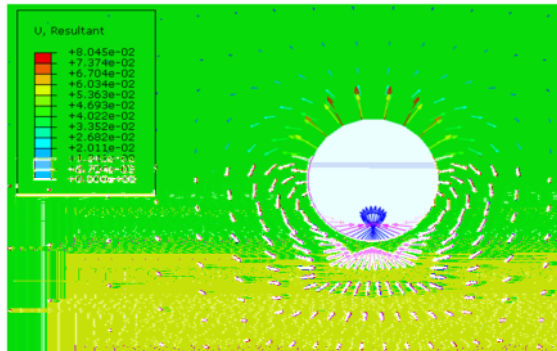
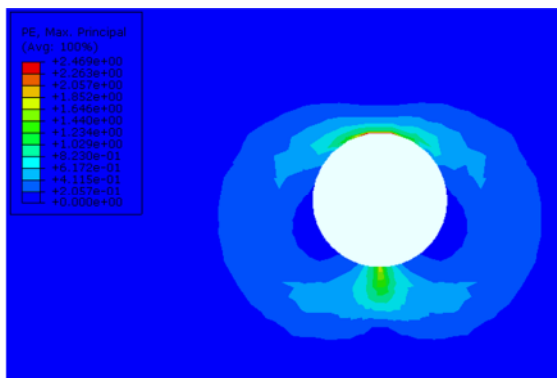


Fig 4: Soil Net Uplift Resistance as a function of Displacement ratio for three different Pipe Embedment Cases

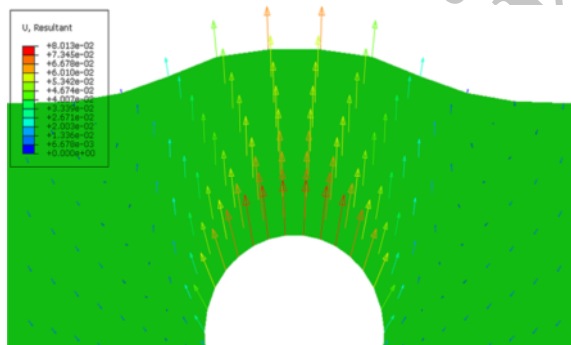


(a) soil displacement around the pipe

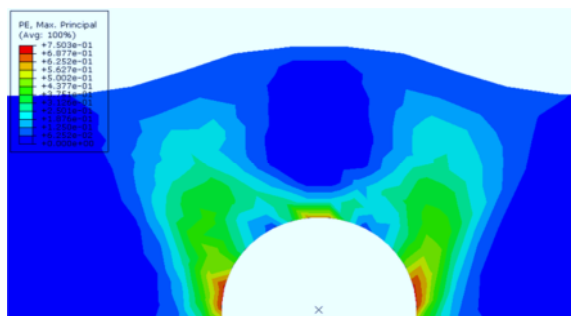


(b) soil plastic strain

Fig. 5 (a): soil displacement around the pipe and (b) soil plastic strain for M-5&M-10 cases



a. soil displacement



b. soil plastic strain

Fig. 6 (a): soil displacement around the pipe and (b) soil plastic strain for M-1 case

#### Excess pore pressure

The change in pore water pressure in the soil below the pipe for M-5 and M-10 is shown in Fig.7. As shown in Fig. 7, negative excess pore pressure was generated beneath the pipe during uplift movement. In addition, excess pore pressure is almost same in both M-5 and M-10. The maximum negative excess pore pressure at highest rate beneath the pipe is about 35 kPa when maximum uplift resistance occurs. As the pipe moves slower, less excess pore pressure generate beneath the pipeline.

The differences between excess pore pressures around pipe confirm that fully consolidated condition has not happened.

#### Effects of pipe rigid body assumption

As mentioned before the pipe is simulated with discrete rigid element. However, to evaluate this assumption on this simulation, the pipe is also modeled as a two dimensional plain stress element. The pipe physical and operational feature is obtained from Northstar Export Line project (Dickin, 1994) internal diameter is equal to 22 centimeters and pipe thickness is assumed 2 centimeter. Finally, pipeline operational pressure is equal to  $10^7$  Pa. The results of uplift resistance toward pipe displacement ratio for both rigid and deformable pipe for M-10 are shown on Fig.8. Excess Pore pressure toward pipe displacement is also depicted in Fig. 9. The result reveals that there is a good convergence between two models. In addition, the amount of elastic strain in pipeline body is also negligible. As a result, rigid assumption of the pipe is correct simplification which provides significant computational savings.

### RESULTS AND DISCUSSION

Comparing the finite element analyses and analytical solutions in the literature has shown consistency between the results. For shallow embedment depth case the finite element analyses indicates that the soil uplift resistance ( $W_u$ ) is equal to 8.9 Kn, while the DNV-OS-F110 for global failure mode give an analytical solution (eq.2) which calculates the amount of uplift resistance equal to 8.6 Kn. This finite element analyses indicates that the normalized vertical force (i.e. uplift factor,  $N_p$ ) is about 10.8 for the deep embedment case (with full bonding). The values of  $N_p$  for an infinite deeply embedded strip plate anchor (fully bonded) have been found to be 10.28 respectively by Rowe and Davis (1982) using bounding plasticity solutions. The results from bounding plasticity solution by Randolph and Houlsby (1984) suggest 11.94 for a rough and fully bonded circular pile. The factor for a smooth pile was found to be 9.14 by Randolph and Houlsby (1984) and the value in practice is usually taken to be an

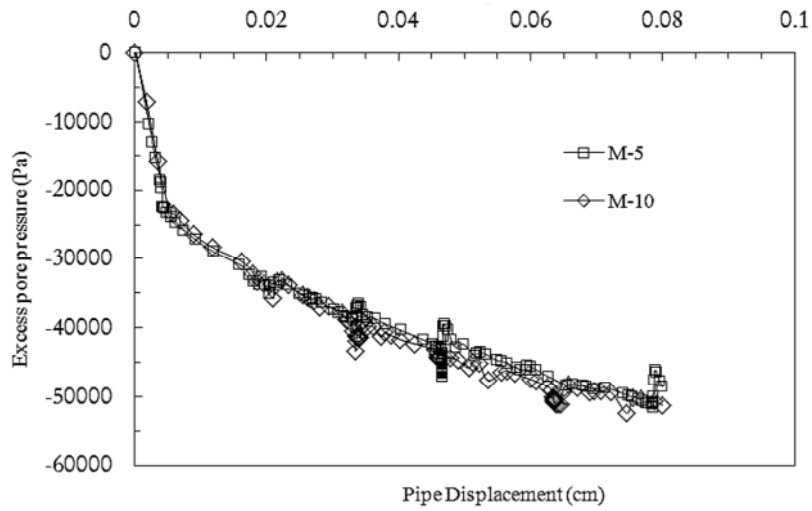


Fig. 7: Excess pore pressure beneath the pipe as a function of Pipe upward Displacement for deep embedment cases (M-5&M-10)

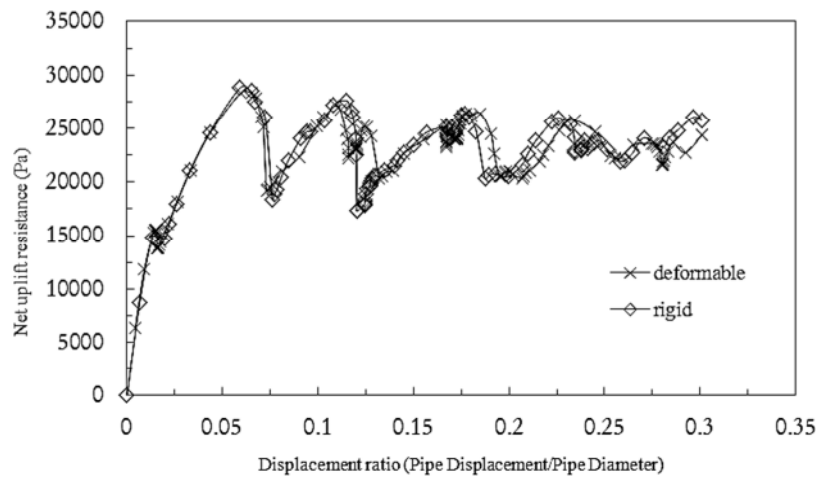


Fig. 8: Effect of Rigid and Deformable pipe assumption on Soil Uplift Resistance for M-10 case

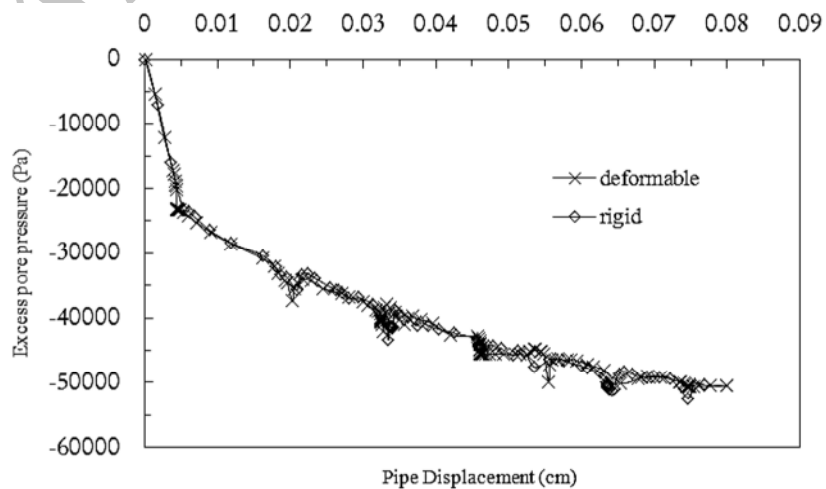


Fig. 9: Effect of Rigid and Deformable pipe assumption on Soil Uplift Resistance for M-10 case

average of the two, i.e. approximately 10.5. In addition, finite element results of Newson and Deljoui (2005) suggests that  $N_c$  is equal to 11.4 for embedment depth of  $H/D=5$ .

The amount of excess pore pressure happens beneath the pipe for very soft clay has been investigated by Thusyanthan *et al.* (2008) and Cheuk *et al.* (2005) through a centrifuge modeling. Both works reveal that negative excess pore pressure appears at bottom of the pipe while pipe move upwards. Similar to these works, ABAQUS/Standard simulation also provides negative excess pore pressure beneath the pipe.

## CONCLUSION

In this paper, the effects of pipeline embedment depth on uplift resistance were investigated. The results show that as embedment depth increases, the uplift resistance also increases substantially. However, for embedment ratio of more than 5 this increase is infinitesimal. In addition, as embedment depth increases, uplift mechanism changes from global failure mode to local failure mode. Soil movement around the pipe demonstrate global failure mode for M-1 in which soil particles move upward toward the pipe. However, in deep embedment cases (M-5, M-10) soil particles flow around the pipe and guaranty local failure mechanism. The results also reveal that negative excess pore pressure would occur beneath the pipe for deep embedment case. This negative pressure does not differ significantly from M-5 to M-10. Moreover, results decode that rigid body simulation of pipeline is a valid simplification. To evaluate this simplification effect on simulation, the pipe is also modeled as a continuum element. The uplift resistance was calculated for both cases and it shows good convergence between two cases. The finite element simulation was validated by both previous experimental and centrifuge works and the results are among the previous findings of this area of science.

## REFERENCES

Bransby, M.; Newson, T.; Brunning, P., (2002). Centrifuge modelling of the upheaval capacity of pipelines in liquefied clay. *Isopie 2002*.  
Bransby, M.F.; N. T. A. B. P., (2002). Physical modelling of the upheaval resistance of buried offshore pipelines. *International conference on physical modelling in geotechnics*. Kitakyushu, Japan.  
Cheuk, C.; Take, W.; Bolton, M.; Oliveira J., (2007). Soil restraint on buckling oil and gas pipelines buried in lumpy clay fill. *Engineering structures*,

29, 973-982.  
Cheuk, C.; White, D.; Bolton, M., (2008a). Uplift mechanisms of pipes buried in sand. *Journal of geotechnical and geoenvironmental engineering*, 134, 154-163.  
Cheuk, C.; White, D.; Bolton, M. D., (2008b). Uplift mechanisms of pipes buried in sand. *Journal of geotechnical and geoenvironmental engineering*, 134, 154-163.  
Dickin, E. A., (1994). Uplift resistance of buried pipelines in sand. *Soils and foundations*, 34, 41-48.  
Dnv (2007). Dnv-rp-f110, global buckling of submarine pipelines det norske veritas.  
Finch, M., (1999). "upheaval buckling and floatation of rigid pipelines": the influence of recent geotechnical research on the current state of the art. *Offshore technology conference*. Houston, texas: offshore technology conference.  
Maltby, T. C.; Calladine, C. R., (1995). An investigation into upheaval buckling of buried pipelines—ii. Theory and analysis of experimental observations. *International journal of mechanical sciences*, 37, 965-983.  
Merifield, R.; White, D.; Randolph, M., (2008). The effect of pipe-soil interface conditions on undrained breakout resistance of partially-embedded pipelines. *Proceedings of the 12th international conference of international association for computer methods and advances in geomechanics*, Goa, India, 1-6.  
Moradi, M.; Craig, W., (1998). Observation of upheaval buckling of buried pipelines. *Proc. Of inter. Conf. Centrifuge*, 98, 693-698.  
Newson, T. A.; Deljoui, P., (2005). Finite element modelling of upheaval buckling of buried offshore pipelines in clayey soils. *Soil and rock behavior and modeling*.  
Randolph, M. F.; Houlsby, G. T. (1984). Limiting pressure on a circular pile loaded laterally in cohesive soil. *Geotechnique*, 34, 613-623.  
Sheng, D.; Nazem, M.; Carter, J. P., (2009). Some computational aspects for solving deep penetration problems in geomechanics. *Computational mechanics*, 44, 549-561.  
Tho, K.; Leung, C.; Chow, Y.; Swaddiwudhipong, S., (2012). Eulerian finite-element technique for analysis of jack-up spudcan penetration. *International journal of geomechanics*, 12, 64-73.  
Thusyanthan, N.; Ganesan, S. A.; Bolton, M. D.; Peter A., (2008). Upheaval buckling resistance of pipelines buried in clayey backfill. *Proceeding of isopie 2008, the eighteenth international offshore and polar engineering conference*, 6-11.

**How to cite this article: (Harvard style)**

*Koochekali, A.; Gatmiri, B.; Koochekali, A., (2013). Pipeline upheaval buckling in clayey backfill using numerical analysis* *Int. J. Mar. Sci. Eng.*, 3 (2), 43-50.

Archive of SID